P3.8 PRECIPITATION AND MICROPHYSICAL CHARACTERISTICS OF OBJECTIVELY DERIVED MCS REGIMES

Mick Pope[1*], Christian Jakob[2], and Michael Reeder[2]

[1]Bureau of Meteorology, Melbourne, Australia
[2]Monash University, Melbourne, Australia

1. INTRODUCTION

Data from the Tropical Rainfall Measuring Mission (TRMM) satellite has been extensively used to study the precipitation, microphysical and lightning characteristics of convection in the tropics (e.g. Cecil et al 2005). The seasonal cycle, geographical variation (including land/sea differences) and diurnal cycle have been examined also (Zipser et al 2006). This study uses precipitation features (PFs) derived from TRMM data (Nesbitt and Zipser 2003) and combines them with information on MCS regimes, which were objectively derived from using an IR tracking algorithm.

Kondo et al (2006) compared TRMM PFs with convective systems from Geostationary Meteorological Satellite (GMS) that were tracked through time over the Maritime Continent for June-August 2000. They found that the maximum rain rate obtained from both the passive microwave (TMI) and precipitation radar (PR) occurred near the time of minimum cloud brightness temperature, which occurs at the beginning of the cloud system lifetime.

The present study matches TRMM PFs from the University of Utah database with Mesoscale Convective Systems (MCSs) identified and tracked using 48 months (six seasons from September to April) of GMS IR1 data over northern Australia and surrounding waters (5-20°S, 120-150°E). MCSs were objectively identified as belonging to one of four regimes based on characteristics derived from the IR data. The precipitation and microphysical characteristics of the PFs from TRMM are grouped into the MCS regimes to better describe the IR regimes derived from the GMS imagery.

* *Corresponding author:* Mick Pope, BMTC, Bureau of Meteorology, PO Box 1289, Melbourne 3000, Victoria, Australia
E-mail: m.pope@bom.gov.au

2. METHODOLOGY

MCSs were identified and tracked throughout their lifetimes using the algorithm of Williams and Houze (1987). A minimum size threshold for tracking of 5000 km^2 together with a minimum MCS lifetime of 2 hours were applied to exclude small and short-lived systems. MCSs that merged during their lifetime are included in the data set.

Five characteristics of the MCSs were used to objectively identify regimes: lifetime, cloudy area expansion rate during first hour after appearance, lifetime minimum cloud top temperature, lifetime maximum size (equivalent radius), and lifetime mean zonal propagation speed based on the centroid of the MCS. The first four of these five parameters are not independent. However, while it may be shown that, for example, there is an approximately linear relationship between the MCS lifetime and the maximum size attained, there is a large spread in the data. All five parameters were retained in the analysis to provide the maximum amount of information about the MCSs.

After normalisation, a K-Means cluster analysis was performed (e.g. Afifi, Clark and May 2004). The optimal solution for MCSs identified using 235 K and 208 K cloud top temperature thresholds revealed four MCS regimes (see below).

PFs of 4 or more pixels from the TRMM precipitation radar were then matched in space and time with the IR-derived MCSs, and identified with a particular MCS regime when the centroid of a PF lay within the MCS. The PFs were taken from the University of Utah TRMM database. The matching was performed only with MCS identified using a 208 K threshold.

3. RESULTS

3.1 MCS regimes

The four MCS regimes identified using the above algorithm are a short-lifetime (Short), long-lifetime (Long), as well as two intermediate-life time regimes. The latter regimes are distinguished by their zonal propagation into westward propagating (Int-W) and eastward propagating (Int-E). MCSs belonging to the Short regime have the shortest lifetimes (95% ≤ 4 hrs), smallest areas (95% have r ≤ 80 km), largest lifetime minimum pixel temperatures (95% have T_{min} ≥ 187K) and weakest expansion rates. Long lifetimes (95% have lifetimes ≥ 4 hrs and 50% ≥ 6 hrs), large size (95% r ≥ 92 km), rapid initial expansion and low lifetime minimum pixel temperatures typify the Long regime. The Int-W and Int-E regimes appear similar to each other in most aspects and are solely distinguished by their direction of propagation. A comparison between the five parameters for each MCS regime is shown in Figure 1.

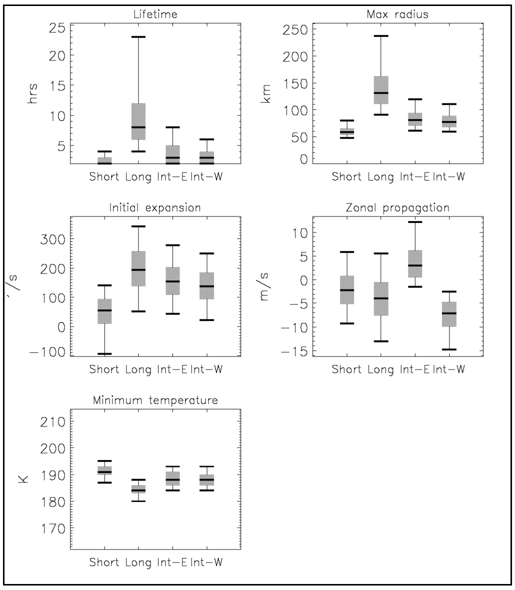

Figure 1. Box-whisker plots of MCS lifetime, maximum lifetime equivalent radius, normalised area expansion rate over the first hour after appearance, mean lifetime zonal propagation velocity of MCS centroid and minimum lifetime temperature for MCS using a 208 K cloud top temperature threshold. The mid-bar indicates the median value, the box 25/75% values and the whickers 5/95% values.

3.2 PF characteristics of MCS regimes

PFs may be classified as containing a MCS when the PF has an 85 GHz 250 K corrected temperature (PCT) area ≥ 2000 km^2, and a minimum PCT ≤ 225 K (Mohr and Zipser 1996). For the Utah TRMM database, this requires 108 250 K pixels pre satellite boost and 82 post-boost, and 10 and 8 225 K pixels respectively pre and post boost. Figure 2 shows probability distribution functions (pdfs) for PFs with no MCS, only containing MCSs and all PFs for each of the four IR MCS regimes.

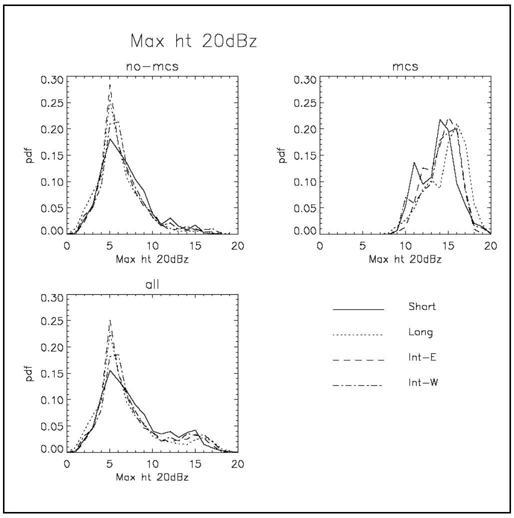

Figure 2. Probability distribution functions for PF matches with IR MCS regimes for the maximum height of the 20 dBz echo. Panels show comparisons between the four regimes for PFs without MCSs (top left), only containing MCSs (top right) and all PFs (bottom left). MCS regimes are indicated by solid (Short), dotted (Long), dashed (Int-E) and dot-dashed (Int-W) lines.

To determine whether or not the differences between PF pdfs for each of the MCS regimes were significant, a two-sided Kolmogorov-Smirnov (KS) test was applied, to test the hypothesis that the data were drawn from the same distribution. For the maximum 20 dBz height, the hypothesis was accepted only for Int-E and Int-W PFs with large ice scattering, i.e. the MCS PFs. All other results were below the 5% confidence interval, and hence the hypothesis was rejected.

The maximum height of the 20 dBz echo is tri-modal with peaks near 5, 11 and 15 km. The 11 and 15 km peaks are mostly from PFs with significant ice scattering. The Long MCS regime has the broadest distribution of 20 dBz heights, including the tallest echoes observed. A similar result is obtained for the maximum height of the 40 dBz echo (not shown). The vast majority of PFs without MCS PFs do not have 40 dBz echoes. As for the 20 dBz threshold, the tallest echoes with heights near 16 km occur in the Long regime. From the above we conclude that updraft strength is related to MCS lifetime.

Figure 3 shows the cumulative probability distribution function for 85 GHz PCTs. The Long regime is more likely to contain pixels lower than ~150 K than the other regimes, with the short regime more likely to contain the larger 85 GHz PCT values. The Int-E and Int-W regimes are similar in distribution for MCS PFs. Int-W and Short are also found to be similar according to the KS test. As with the maximum reflectivity heights, there is evidence for a relationship with the MCS lifetime, with the longer lived systems producing large ice scattering during their lifetimes.

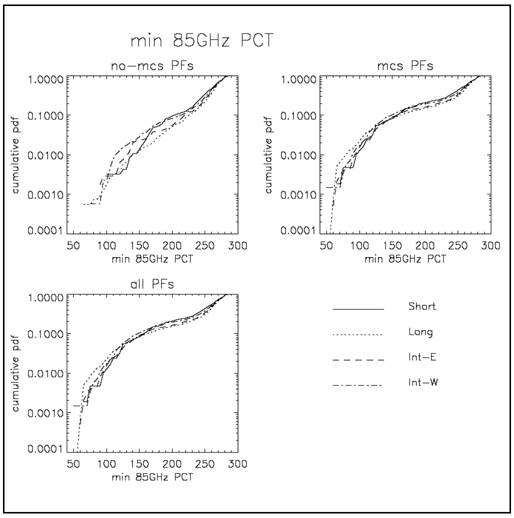

Figure 3. Cumulative probability distribution functions for PF matches with IR MCS regimes for the minimum 85 GHz PCT.

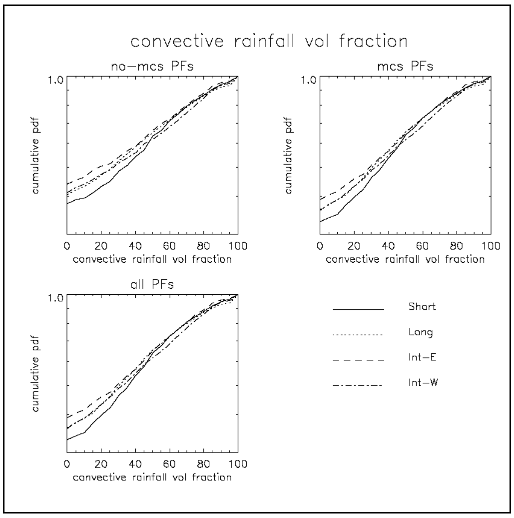

Figure 4. Cumulative probability distribution functions for PF matches with IR MCS regimes for the maximum height of the 40 dBz echo.

Figure 4 shows the cumulative distribution function for the fraction of precipitation identified as convective. The Short regime is the regime most likely to have the largest convective rainfall fraction. This regime represents small, short-lived MCS (within the imposed limits of 5000 km^2 and 2 hour lifetime) with the warmest cloud tops (Figure 1). As such systems usually exhibit only small anvils the amount of stratiform rain in them is relatively small, leading to the relatively higher convective rainfall fractions seen in Figure 4.

3.3 Evolution of PF characteristics

A major strength of combining the IR-derived MCS data with the TRMM PFs is that it allows the construction of the composite time evolution of PF properties across the MCS lifetime. For this purpose the MCS lifetime was split into a growth, mature and decay phase. The results for the minimum 85 GHz PCT and maximum 20 dBz heights for all PFs is shown in Figures 5 and 6.

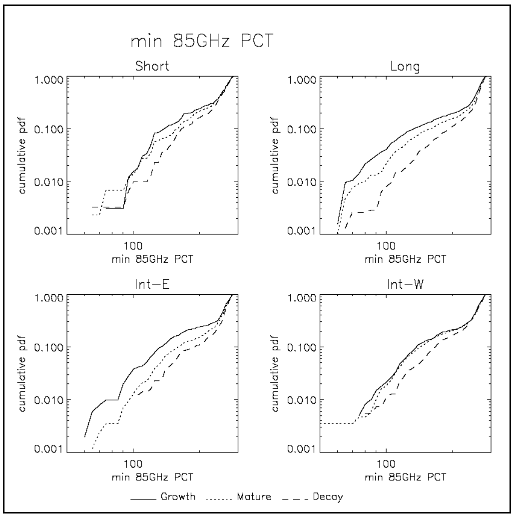

Figure 5. Cumulative probability distribution functions for the minimum 85 GHz PCT for all PFs for each of the four IR MCS regimes for the three stages of MCS evolution, growth (solid line), mature phase (dotted) and decay (dashed).

The hypothesis that the PF distributions for each stage of the MCS's lifetime are drawn from the same distribution was accepted for Short and Int-W. This result in unsurprising given that 95% of all MCSs have lifetimes ≤ 4 hrs for the Short regime and ≤ 6 hrs for the Int-W regime. The strongest ice scattering as evidenced from the 85 GHZ temperatures occurs in the growth phase of the MCS. This is also the time of the largest convective cloud fraction and largest number of cold 85 GHz pixels (not shown).

The distributions of maximum 20 dBz heights are bi-modal with heights near 5 km and 15-17 km. This latter peak was shown earlier to be due to MCS PFs, i.e. those with large ice scattering. This peak is largest during the growth phase. The peak near 5 km typically becomes broader as the MCS ages in the case of Short (where it broadens towards larger values), Long (towards smaller tops) and Int-W. The Int-E regime peak becomes more significant at 5km. As for 85 GHz, only the results for the Long and Int-E regimes are statistically significant according to the KS test.

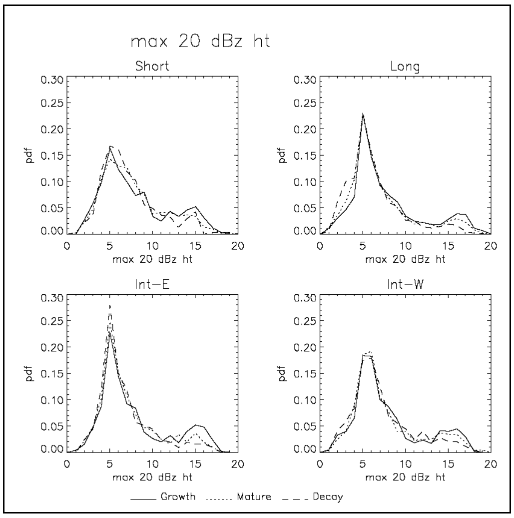

Figure 6. Probability distribution functions of the maximum 20 dBz heights for all PFs for each of the four IR MCS regimes for the three stages of MCS evolution, growth (solid line), mature phase (dotted) and decay (dashed).

4. CONCLUSIONS

Precipitation features from the University of Utah TRMM database were matched with MCSs identified from IR data using 208 K as the temperature threshold. PF distributions were compared for three PF datasets: those containing a PF MCS defined by 85 GHz parameters, those without such a MCS and all PFs. In general, the Long regime MCS were found to have the tallest 20 and 40 dBz echoes and smallest minimum 85 GHz PCT values, consistent with having the strongest updrafts. The Short regime had values consistent with weaker updrafts. For the MCS PFs, the two Intermediate regimes were indistinguishable. It appears that MCS lifetime is related to updraft strength. Temporal variations were observed in 20 dBz maximum height and minimum 85 GHz PCT. For the Long and Int-E regime, it was found that heights decrease and 85 GHz values increase during the MCS lifetime. Hence, it is likely that the strongest updrafts occur during the growth phase, and contribute to the MCS lifetime. This is consistent with the result that the Long regime has the largest initial area expansion rate and the Short regime the smallest. Machado and Laurent (2004) found that the initial expansion rate was a reasonable predictor of MCS lifetime over South America, and has been confirmed over northern Australia (Pope, unpublished results).

Acknowledgements
The authors thank Chuntao Liu and Ed Zipser for use of the University of Utah TRMM dataset. Mick Pope acknowledges the support of a Bureau of Meteorology scholarship.

REFERENCES

Afifi, A., V.A. Clark, and S. May, 2004: Computer-Aided Multivariate Analysis, Chapman and Hall/CRC, Boea Raton, Fl, 489pp.

Cecil, D. J., S. J. Goodman, D. J. Boccippio, E. J. Zipser, and S. W. Nesbitt, 2005: Three years of TRMM precipitation features. Part I: Radar, radiometric, land lightning characteristics. *Mon. Wea. Rev.*, **133**, 543-566.

Kondo, Y., A. Higuchi, and K. Nakamura, 2006: Small-scale cloud activity over the Maritime Continent and the Western Pacific as revealed by satellite data. *Mon. Wea. Rev.*, **134**, 1581–1599.

Machado, L.A.T., and H. Laurent, 2004: The Convective System Area Expansion over Amazonia and Its Relationships with Convective System Life Duration and High-Level Wind Divergence, *Mon. Wea. Rev.,* **132**, 714-725.

Nesbitt, S.W., and E.J. Zipser, 2003: The diurnal cycle of rainfall and convective intensity according to three years of TRMM measurements. *J. Climate*, **16**, 1456–1475.

Williams, M. and R.A. Houze Jr., 1987: Satellite-observed characteristics of winter monsoon cloud clusters, *Mon. Wea. Rev.,* **115**, 505-519.

Zipser, E.J., D. J. Cecil, C. Liu, S. W. Nesbitt and D. P. Yorty, 2006: Where are the most intense thunderstorms on earth? *Bull. Amer. Meteor. Soc.*, **87**, 1057–1071.